Research article

Dynamics of urban expansion and form changes impacting carbon emissions in the Guangdong-Hong Kong-Macao Greater Bay Area counties

Lei Ming [a,b,c], Yuandong Wang [a,b,c,*], Xiaojie Chen [a,b], Lihong Meng [a,b,d]

[a] School of Geography and Environmental Engineering, Gannan Normal University, Ganzhou, 341000, China
[b] Jiangxi Provincial Key Laboratory of Urban Solid Waste Low Carbon Circulation Technology, Ganzhou, 341000, China
[c] Institute of National Land Space Planning, Gannan Normal University, China
[d] Basic Geography Experimental Center, Gannan Normal University, China

A B S T R A C T

Cities are the main carriers of social and economic development, and they are also important sources of carbon emissions. Therefore, it is essential to explore the impact of urban expansion and form changes on carbon emissions. Here, we attempted to analyzes the relationship between urban expansion and carbon emissions at the county level in the Guangdong-Hong Kong-Macao Greater Bay Area (GBA) from 1997 to 2017. It further decomposes the driving effects of carbon emissions from multiple factors, and considers the spatial heterogeneity between different urban form changes and driving effects. The results show that: The relationship between urban expansion and carbon emissions in the GBA has gone through three stages from 1997 to 2017, with 2012 as a turning point. Optimization of economic development models and strict protection of the ecological environment can effectively control carbon emissions. After 2012, the economic development effect (GE) and population scale effect (PE) are the driving factors of carbon emissions, while the carbon emission intensity effect (CE) and urban land intensity effect (UE) are the inhibitory factors of carbon emissions. The contribution rate of UE to carbon emission reduction can reach 86 %. The impact of urban form changes on carbon emissions has spatial heterogeneity. The changes in urban form have a significant impact on the carbon emissions of counties in Dongguan and Shenzhen. The increase in fragmentation indirectly promotes carbon emissions. In 2007–2012, the increase in centrality significantly weakened the economic development effect, which is conducive to emission reduction. After 2007, the increase in compactness in counties in the eastern part of the GBA, including Zhongshan and Zhuhai, is not conducive to emission reduction.

1. Introduction

Over the past few decades, China has experienced rapid urbanization and industrialization, resulting in a significant increase in urban construction land [1,2]. Consequently, such expansive urban growth has given rise to various ecological and environmental issues [3], with particular attention given to the correlation between urban expansion and carbon emissions [4,5].

The urban metamorphosis that China has undergone has intrinsically linked urban sprawl to carbon emissions. Time-series analysis using multi-source remote sensing data underscores the enlargement of urban territories in major cities, which correlates with a surge in carbon emissions. This relationship, however, isn't merely linear but intricately layered [6–8]. Various determinants, such as economic trajectories, population flux, and industrial shifts, influence urban growth [9–12]. Interestingly, these determinants also play a pivotal role in shaping urban carbon footprints [13,14].

Remote sensing insights reveal that the urban sprawl reshapes land use paradigms, diminishing soil organic carbon reserves while amplifying biomass carbon stocks [15]. Urban centers, in their burgeoning phase, evolve as dominant hubs of socio-economic activities. Yet, this rapid ascent often necessitates heightened fossil energy consumption, escalating carbon emissions [16–18]. While a general positive link between urban sprawl and carbon emissions is acknowledged [19,20], it's imperative to understand that regional specificities can alter the intensity of this linkage [21].

Further exploration into the nexus between urban expansion and carbon emissions reveals the role of evolving urban forms. These urban forms, typically inferred from remote sensing data, are in constant flux as cities expand, each change exerting different impacts on carbon emissions [22–24]. For instance, studies in regions like the Yangtze and Pearl River Deltas suggest that cities with compact layouts tend to have lower emissions [25]. On a broader scale, the compactness of urban forms and their relationship with carbon emissions present a layered narrative, with pivotal threshold points emerging as critical variables [26]. Notably, the dynamics of urban forms in Chinese cities correlate with CO_2 emissions, a relationship that intensifies with population growth [27]. Given these observations, considering urban form dynamics in urban development can refine urban planning strategies, influencing carbon emissions [28].

Currently, there has been a wealth of research on the relationship between urban expansion and form changes and carbon emissions. These studies have revealed a more in-depth nonlinear relationship between the two [29,30]. While a large number of studies have explored the key factors that drive carbon emissions [31], and it is also recognized that urban form changes have an important impact on carbon emissions during urban expansion [32], there is a lack of understanding of the complex relationship between urban expansion and form changes and carbon emissions under the driving of multiple factors. Therefore, it is necessary to understand the relationship between urban expansion and carbon emissions, analyze the driving factors of carbon emissions, and explore the impact of urban form changes on the driving effects of different factors on carbon emissions.

This study focuses on the Guangdong-Hong Kong-Macao Greater Bay Area (GBA), which has experienced rapid urban expansion and is one of the regions with the most significant growth in carbon emissions. The region also has significant development disparities.
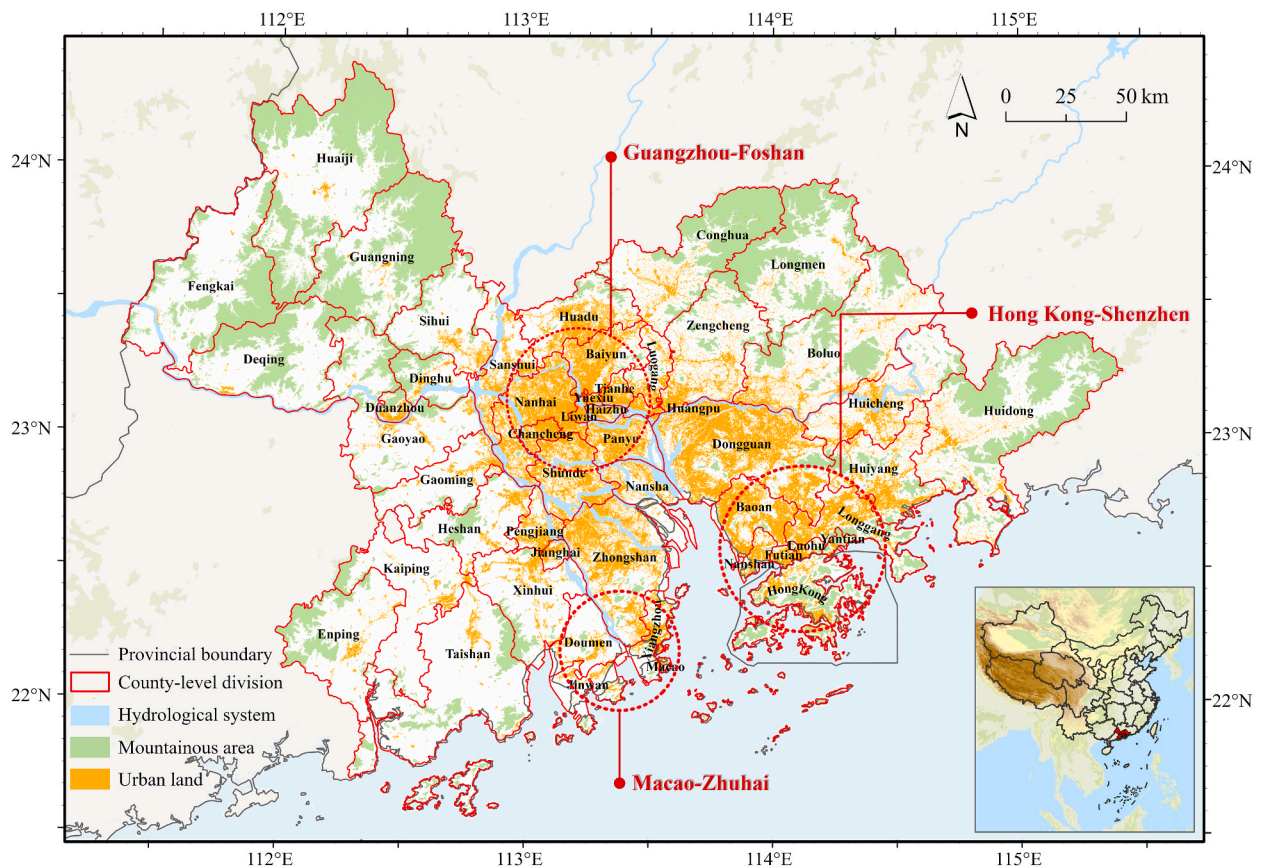

Fig. 1. Study area diagram.

Using multi-source remote sensing data products and related statistical information, the study aims to understand the spatio-temporal relationship between county-level urban expansion and carbon emissions. Using an improved LMDI model, the study identifies the driving effects of multiple factors on carbon emissions, and uses MGWR to test the spatial heterogeneity between urban form changes and different carbon emissions driving effects. The overall goal is to provide theoretical guidance and insights for carbon neutrality in the GBA.

2. Study area and data sources

2.1. Study area

Our research focuses on the Guangdong-Hong Kong-Macao Greater Bay Area (GBA),encompasses the Hong Kong、Macao and a selection of cities from Guangdong Province, including Guangzhou, Shenzhen, Foshan, Dongguan, Zhuhai, Huizhou, Zhongshan, Jiangmen, and Zhaoqing (Fig. 1). The GBA has a land area of 55,900 square kilometers, a total population of 86.69 million at the end of 2021, and a gross regional product of over 12 trillion yuan. It is one of the regions with the strongest economic strength, innovation capacity, and development vitality in China. After the rapid development since the reform and opening up, the GBA has become the city cluster with the highest per capita GDP and economic density in China. In the 20 years from 1997 to 2017, the urban land area of the GBA increased by 6114.08 square kilometers, while the total carbon emissions increased from 117.45 million tons in 1997 to 326.32 million tons in 2017. Rapid urbanization has brought about the prosperity and rapid development of the regional economy, but this expansion is accompanied by high-intensity carbon emissions, which is unsustainable. It will also lead to a series of environmental problems, threatening the sustainable development of the GBA. It is urgent to explore in depth the impact of urbanization in the GBA on carbon emissions.

2.2. Data sources

To ensure the completeness and accuracy of the data, and considering the differences in data statistical caliber and data sources between the Mainland and the Hong Kong and Macao Special Administrative Regions, this study takes the 48 counties of the GBA in 2013 as the research unit, including counties, districts, county-level cities, as well as two municipal towns, Dongguan and Zhongshan.

The experimental data in this paper includes carbon emission data, urban land use data, population data, and economic data in the study area from 1997 to 2017.

The county-level carbon emission data from 1997 to 2017 are from the China Carbon Emissions Database (CEADs). The carbon emission data provided by CEADs use the particle swarm optimization backpropagation (PSO-BP) algorithm to unify the proportions of DMSP/OLS and NPP/VIIRS satellite images, and estimate the carbon dioxide emissions of 2735 counties in China from 1997 to 2017. It has the advantages of wide coverage and long time span [33].

The urban built-up land data from 1997 to 2017 comes from the Global Artificial Impervious Surfaces (GAIA) dataset. This dataset uses Landsat images to create annual maps of high-resolution global artificial impervious areas over 30 years on the GEE platform. The average overall accuracy is above 90 %, with a resolution of 30 m × 30 m [34]. GEE provides the dataset (Tsinghua/-FROM-GLC/GAIA/v10). This paper used this data to count the area of urban built-up land in each county.

The population data comes from Worldpop (www.worldpop.org). This data can be obtained in Google Earth Engine (GEE) (WorldPop/GP/100 m/pop). It uses machine learning methods to establish the relationship between population density and a series of geospatial covariate layers, and provides global population distribution data from 2000 to 2021 with a resolution of 100 m × 100 m [35]. This paper counted the total population of each county in the study area in GEE, and supplemented the population data from 1997 to 1999 using the trend line fitting method.

The economic data from 1997 to 2017 is the Global Electricity Consumption GDP dataset. It uses the calibrated nighttime light data and a top-down approach to calculate the corrected real GDP and electricity consumption of global 1-km × 1-km grids from 1992 to 2019 [36]. This data has the advantages of wide coverage and long time span, and can also be obtained on GEE (projects/sat-io/open-datasets/GRIDDED_EC). This paper based on this data to count the GDP data of each county.

3. Methods

3.1. Tapio decoupling model

"Decoupling" refers to the concept of reducing environmental pressure or resource consumption associated with economic growth. Tapio originally studied the decoupling state of the European transport industry by examining elasticity coefficients and classifying the different decoupling states [37]. In recent years, this model has been widely used to explore the relationship between energy consumption, environmental pollution, and economic growth [38] [–] [40]. This also includes the relationship between urbanization and carbon emissions. Using the Tapio decoupling model can more finely depict the decoupling state of the two, and examine whether the development status of the two is unbalanced [5,41]. Therefore, this paper adopts the Tapio decoupling model to explore the relationship between urban expansion and carbon emissions in the GBA, and understand the decoupling state between the two. The computational model is shown in Eq. (1):

$$T = \frac{\frac{\Delta C}{C_0}}{\frac{\Delta U}{U_0}} = \frac{(C_t - C_0)/C_0}{(U_t - U_0)/U_0} \tag{1}$$

where T denotes the decoupling index, C_0 and U_0 represent the initial carbon emissions and urban land area respectively, C_t and U_t denote the final carbon emissions and urban land area respectively, ΔC indicates the change in carbon emissions over this period, and ΔU indicates the change in urban construction land over this period.

According to existing literature, there are three types of decoupling states, decoupling, coupling, and negative decoupling. These can be further divided into eight degrees of decoupling, as shown in Table 1.

3.2. 3.2 extended LMDI model

The extended LMDI decompose model is based on the extended Kaya identity and the LMDI decompose model [42]. The Kaya identity is often used by the Intergovernmental Panel on Climate Change (IPCC) to analyze emission drivers [39]. The LMDI decompose model is a type of index decomposition analysis (IDA) method [43]. Studies have shown that the LMDI decompose model has the advantages of being easy to interpret results and having no residuals [44]. Therefore, using the extended LMDI decompose model can quantify the contributions of multiple factors to carbon emissions [45,46].

First, the carbon emission model of the GBA is established based on the Kaya equation, decomposing carbon emissions into four key drivers, as shown in Eq. (2).

$$C = \frac{C}{GDP} \times \frac{GDP}{U} \times \frac{U}{P} \times P = CG \times GU \times UP \times PO \tag{2}$$

where C denotes total carbon emissions, GDP represents gross regional product, U indicates urban land area, and P refers to total population. CG = C/GDP, representing carbon emission intensity, GU = GDP/U, indicating urban economic density, UP＝U/P, reflecting per capita urban land area, P＝PO, representing population scale.

Then, leveraging the LMDI decomposition methodology, the contribution of each driver to carbon emission changes ΔC can be quantified as Eq. (3):

$$\Delta C = C_t - C_0 = \Delta C_{CG} + \Delta C_{GU} + \Delta C_{UP} + \Delta C_{PO} \tag{3}$$

The terms on the right-hand side of Eq. (3) are calculated as follows Eqs. (4)–(7):

$$\Delta C_{CG} = \frac{C_t - C_0}{\ln C_t - \ln C_0} \ln\left(\frac{CG_t}{CG_0}\right) \tag{4}$$

$$\Delta C_{CG} = \frac{C_t - C_0}{\ln C_t - \ln C_0} \ln\left(\frac{CG_t}{CG_0}\right) \tag{5}$$

$$\Delta C_{UP} = \frac{C_t - C_0}{\ln C_t - \ln C_0} \ln\left(\frac{UP_t}{UP_0}\right) \tag{6}$$

$$\Delta C_{PO} = \frac{C_t - C_0}{\ln C_t - \ln C_0} \ln\left(\frac{PO_t}{PO_0}\right) \tag{7}$$

In the above formula, ΔC_{CG} denotes the carbon intensity effect, reflecting the regional economy's carbon dependence, abbreviated as CE; ΔC_{GU} represents the economic growth effect, indicating urban economic growth impacts on emissions, abbreviated as GE; ΔC_{UP} reflects the urban land intensity effect, capturing land use efficiency influences on emissions, abbreviated as UE; ΔC_{PO} embodies the population scale effect, showing the emissions impact of population size, abbreviated as PE.

Table 1
Tapio decoupling state partition.

Degree	ΔC	ΔU	T
Strong decoupling	<0	>0	T < 0
Weak decoupling	>0	>0	0<T < 0.8
Recessive decoupling	<0	<0	T > 1.2
Expansive coupling	>0	>0	0.8<T < 1.2
Recessive coupling	<0	<0	0.8<T < 1.2
Strong negative decoupling	>0	<0	T < 0
Weak negative decoupling	<0	<0	0.8<T < 1.2
Expansive negative decoupling	>0	>0	T > 1.2

Notes: ΔC denotes the change in carbon emissions, ΔU denotes the change in urban land area, and T denotes the decoupling index.

3.3. Characterization of urban form

Urban form is characterized by landscape pattern indices. Landscape pattern indices describe the complexity of landscape patch types and arrangements by combining characteristics such as patch shape, size, number, and spatial combination. They can scientifically characterize urban form [27,47]. Urban landscape indices are based on urban land use and calculated using impervious surface data [48]. Four key landscape pattern indices are selected to measure urban form changes across the GBA during four distinct periods: 1997–2002, 2002–2007, 2007–2012, and 2012–2017. The chosen indicators are as follows (Table 2). In the following text, the change in fragmentation is denoted by ΔNP, the change in centrality by ΔLPI, the change in compactness by ΔCOHESION, and the change in complexity by ΔPARA-MN. These four indicators will be used to explain the drivers of carbon emissions.

3.4. 3.4 MGWR model

The MGWR method was proposed by Fotheringham. Compared with traditional GWR, MGWR can better describe the relationship patterns between variables and explanatory variables in space and across different scales [49]. Based on previous studies [50,51], this paper employs MGWR model to examine scale and spatial variations in the connections between county-level carbon emissions drivers and urban form changes across the GBA. Four carbon emission drivers and four urban form change indicators will be used to explore the impact of urban form change on carbon emissions during urban expansion. The model expression is as follows Eq. (8):

$$Y_i = \sum_{j=1}^{k} \beta_{bij}(u_i, v_i)x_{ij} + \varepsilon_i \tag{8}$$

Where β_{bij} denotes the local regression coefficient; bij signifies the bandwidth utilized for the regression coefficient of variable j; (u_i, v_i) symbolizes the spatial coordinates of sampling site i; x_{ij} refers to the observed measurement of variable j at sampling site i; ε_i r is the random error term. In the MGWR model, each regression coefficient β_{bij} is derived via localized regression, and the bandwidth possesses specificity to each variable.

4. Results

4.1. Spatiotemporal patterns of carbon emissions

Fig. 2 depicts the changes in average county-level carbon emissions for each city in the GBA from 1997 to 2017. Between 1997 and 2002, the growth was relatively slow for all cities except Dongguan and Zhongshan, with Dongguan leading and Zhaoqing lagging. From 2003 to 2012, emissions underwent a significant upward trend, accumulating a 53.8 Mt increase and widening the gap between counties. The cumulative average peaked at 117.9 Mt in 2012. From 2013 to 2017, the average emissions remained relatively stable, with Dongguan and Shenzhen experiencing a downward trend.

Fig. 3 reveals distinct stages in the evolution of each city's county-level average emission sequences through temporal clustering analysis. Between 1997 and 2005, emissions remained low, reflecting a modest environmental impact. A notable rise occurred in 2006–2009, indicating heightened pressure. However, the most significant cluster emerged in 2010–2017, representing a period of sustained high emissions. Overall, adjacent years tend to group together, suggesting relative stability in emission trends. Intriguingly, the 2015–2017 county-level averages resemble those of 2010. This temporal similarity could be linked to China's post-18th Party Congress emphasis on green, low-carbon development, which substantially slowed emission growth.

4.2. Analysis of decoupling state evolution

4.2.1. Temporal evolution of decoupling states

Fig. 4 shows a dynamic trajectory of decoupling states in GBA counties. Individual counties experienced three distinct stages of decoupling, from strong decoupling to expansive negative decoupling, and then back to strong decoupling. Between 1998 and 2006, extensive negative decoupling prevailed, with most counties witnessing uniform levels. Across the region, urban growth outpaced expansion, driving up emissions. During 2007–2011, county decoupling states diverged. Secondary core counties distant from the Pearl River Estuary embraced weak decoupling and even expansive coupling, indicating a shift towards greener urban models unlike the high-emission expansion near the Estuary. From 2012 to 2017, strong decoupling reigned, signaling emissions falling below urban growth rates. Notably, in 2012, several counties within the "Guangzhou-Foshan" and "Hong Kong-Shenzhen" groups lingered in

Table 2
Urban form index and its description.

| Indicator	Landscape pattern index	Abbreviation	Description
Fragmentation	Number of Patches	NP	Measures the degree of dispersion of urban form, value range: NP $\geq$ 1
Centrality	Largest Patch Index	LPI	Reflects the core advantage of urban form, value range: 0<LPI≤100
Compactness	Patch Cohesion Index	COHESION	Reflects the connectivity of urban form, value range: 0≤COHESION≤100
Complexity	Mean Perimeter Area Ratio	PARA - MN	Measures the irregularity of urban form, value range: PARA-MN>0
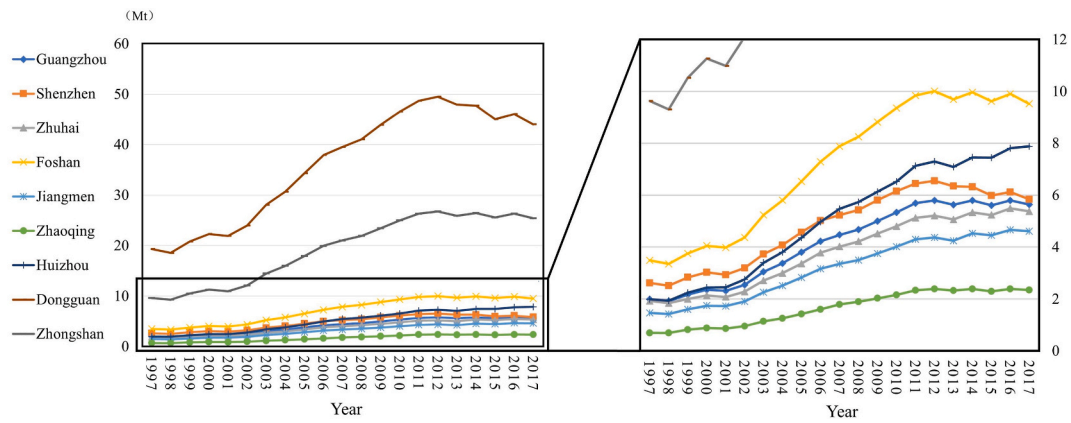
Fig. 2. Average county-level carbon emissions of cities in the GBA from 1997 to 2017.
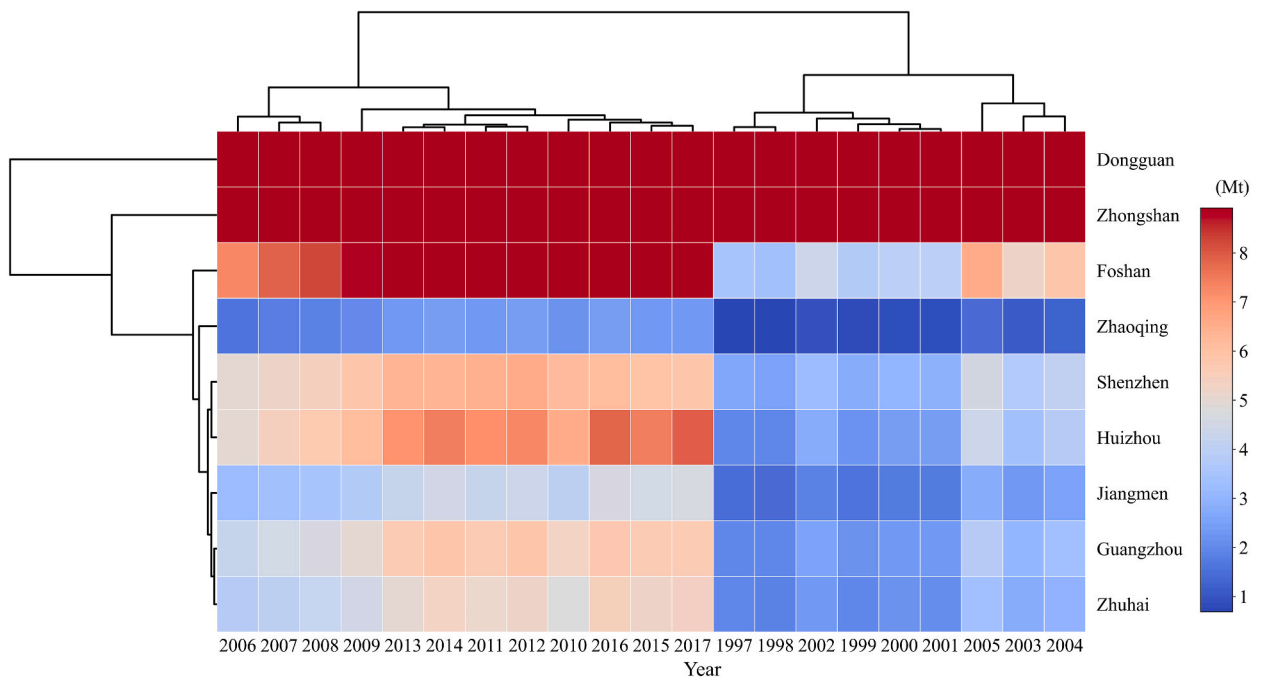

Fig. 3. K-means clustering results of average carbon emissions in counties of each city in the GBA.

expansive negative decoupling, while others transitioned out. By 2013, all counties achieved strong decoupling, reflecting the adoption of the new development philosophy prioritizing low-carbon practices and environmental protection. This marked a transition towards high-quality development in the GBA, characterized by more rational urban expansion and decelerating emissions.

4.2.2. Evolution of decoupling state spatial pattern

The spatial distribution of decoupling states between carbon emissions and urban expansion from 1997 to 2017 is shown in Fig. 5. Between 1997 and 2002 (Fig. 5a), county-level decoupling transitioned from weak to expansive negative decoupling, concentrated around the Pearl River Delta. This shift stemmed from two factors: relatively low regional urbanization and economic development, and higher carbon emission costs in outlying counties due to their location. All counties experienced expansive negative decoupling in 2002–2007 (Fig. 5b), where rapid urban expansion outpaced emission reduction. However, from 2007 to 2012 (Fig. 5c), diverse trends emerged within the "Hong Kong-Shenzhen", "Guangzhou-Foshan", and "Macao-Zhuhai" groups. Differences in economic growth and urbanization patterns led some counties to retain expansive negative decoupling, while others shifted towards weak decoupling and even expansive coupling. In 2012–2017 (Fig. 5d), a breakthrough occurred: all counties escaped expansive negative decoupling, propelling the entire Pearl River Estuary Bay Area into a strong decoupling state. This signified that emission reduction outpaced urban expansion, marking significant progress in low-carbon development. Notably, the northwestern region, designated as a water
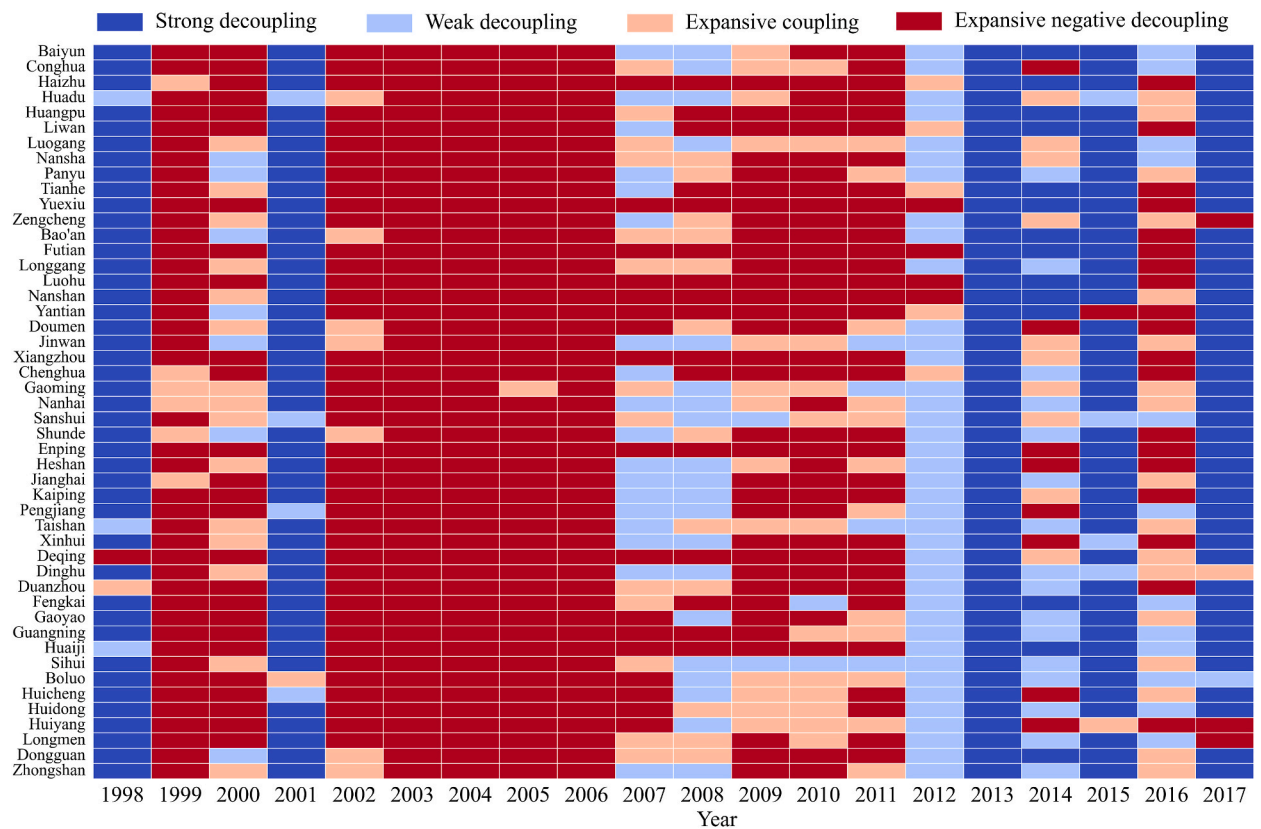
Fig. 4. The decoupling status of counties in the GBA in each year (1998 refers to 1997–1998).

conservation area, contributes uniquely to the Bay Area's ecological protection.

4.3. Decomposition of carbon emissions

Fig. 6 depicts the contributions of various factors to carbon emissions over time, highlighting growing differentiation between driving and inhibiting effects. These factors have become increasingly distinguishable in terms of their positive driving or negative inhibiting effects on carbon emissions.

As shown in Fig. 6a, between 1997 and 2002, there were significant regional differences in carbon emissions among counties in the GBA. PE had a positive driving effect on carbon emissions across the region, with the top three contributing counties being Bao'an, Longmen, and Shunde, with contributions of 2.47, 1.81, and 1.60, respectively. GE was the second-leading driver of carbon emissions, with more than 60 % of counties' carbon emissions being driven by GE, with the most significant impact being in Longmen, with a contribution of 6.97. More than half of the counties' carbon emissions were driven by CE. UE had the most widespread inhibitory effect, with 66 % of counties having UE contributions less than zero. For most counties, under low-carbon emission scenarios, the contributions of the various factors offset each other, and the total contribution was hovering around zero.

As shown in Fig. 6b, between 2002 and 2007, the total contribution of carbon emission driving factors in the GBA was greater than zero, with an average of 2.35 at the county level. The top three counties with the highest total contributions were Dongguan, Zhongshan, and Nansha, with contributions of 15.60, 8.92, and 6.68, respectively. The disparities in carbon emissions between counties widened significantly, and CE and PE were both positive driving factors across the region, with economic development relying on high-carbon emissions and population growth promoting carbon emissions growth. It is worth noting that GE had a relatively widespread inhibitory effect in this period, with 63 % of counties having contributions less than zero, with the most significant being Fengkai, Huaiji, and Baiyun, with contributions of −8.05, −5.02, and −3.64, respectively.

As shown in Fig. 6c, the total contribution of carbon emission driving factors decreased slightly, with an average of 1.56 at the county level. The top three counties with the highest total contributions were Dongguan, Zhongshan, and Nansha, with contributions of 9.96, 5.73, and 3.92, respectively. PE continued to drive carbon emissions across the region, and GE also showed a relatively widespread driving effect, with 71 % of counties' carbon emissions being driven by GE. CE and UE had a wider inhibitory effect on carbon emissions, respectively inhibiting the growth of carbon emissions in 83 % and 65 % of counties. This indicates that the GBA's economic development is becoming less reliant on carbon emissions, and that rational urban land planning can effectively mitigate carbon emissions.
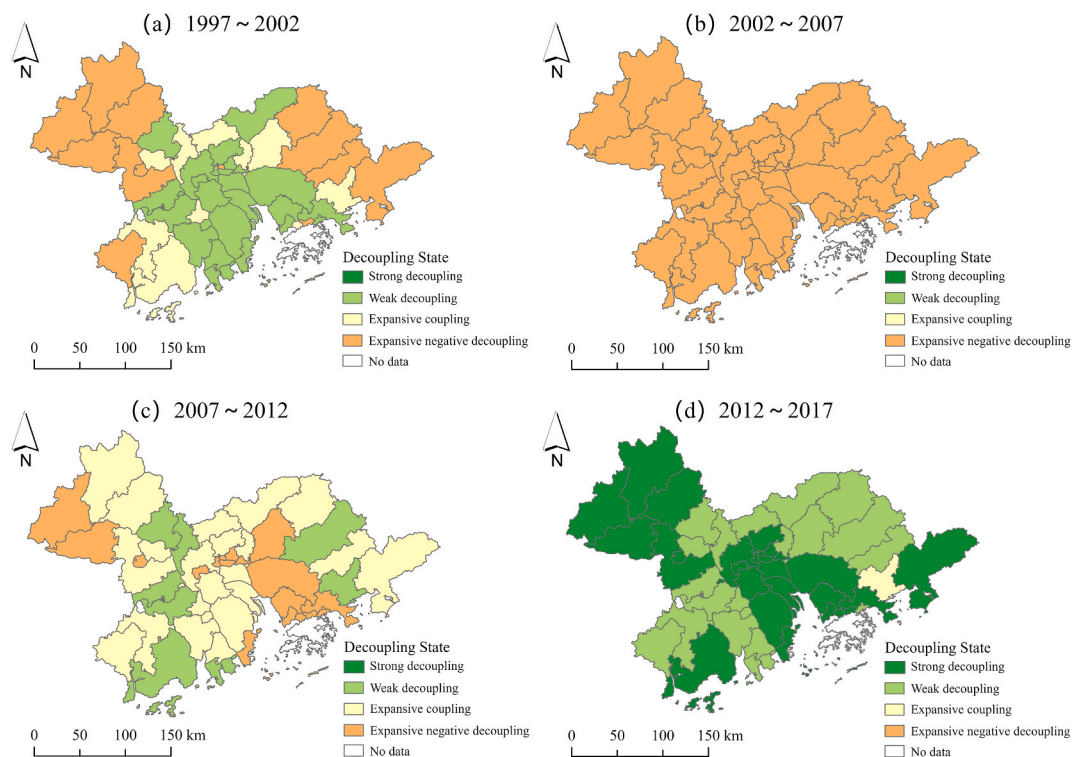
Fig. 5. The spatial distribution of decoupling states between carbon emissions and urban expansion from 1997 to 2017. (a)–(d) are spatial distribution of decoupling states in 1997–2002 (a), 2002–2007 (b), 2007–2012 (c), and 2012–2017 (d).

As shown in Fig. 6d, the four factors showed a clear differentiation, with GE and PE driving carbon emissions, while CE and UE inhibiting carbon emissions. Overall, the inhibitory effect was greater than the driving effect, with the average total contribution of counties at −0.22. The top three counties with the highest total contributions were Jianghai, Xinhui, and Zengcheng, with contributions of 1.96, 1.05, and 0.91, respectively. The bottom three counties were Dongguan, Bao'an, and Baiyun, with contributions of −5.49, −2.19, and −1.46, respectively. Dongguan and Zhongshan had the most significant changes in this period, with their carbon emissions mitigation attributed to the strong inhibitory effect of UE, with contributions of −48.24 and −32.98, respectively. This step shows that rational urban expansion plays an important role in mitigating carbon emissions.

4.4. Urban form changes

The changes in urban form of the counties in the GBA are shown in Fig. 7.

The change in the NP of urban forms in counties showed little difference across different periods, but exhibited strong spatial differences (Fig. 7a). From the perspective of the cumulative changes in four periods, 48 % of counties had a decreasing NP, while 52 % of counties had an increasing NP. The top three counties with the largest cumulative changes were Boluo, Huidong, and Zengcheng, with changes of 7,626, 4,212, and 2,983, respectively. The bottom three counties were Dongguan, Bao'an, and Longgang, with cumulative changes of −10,804, −4,832, and −3,366, respectively. This indicates that the degree of dispersion of urban land in counties is heading in different directions, reflecting different urban development patterns in different regions.

From the perspective of the change in the LPI of urban forms, the LPI of all counties increased in the four periods (Fig. 7b). The top three counties with the largest cumulative changes were Baiyun, Liwan, and Panyu, with changes of 41.44, 39.69, and 35.56, respectively. The bottom three counties were Fengkai, Huaiji, and Guangning, with changes of 0.05, 0.09, and 0.12, respectively. This shows that the difference in the advantage of the urban cores of counties in the GBA is very large, and there are huge differences in the way of urban expansion.

In the change of the COHESION of urban forms, there are large spatial differences (Fig. 7c). In general, the COHESION of most counties is increasing. From the perspective of the cumulative changes in four periods, only Yuexiu is decreasing, with a change of −0.01. The top three counties with the largest cumulative changes are Jinwan, Boluo, and Longmen, with changes of 8.70, 7.79, and 7.45, respectively. This indicates that the urban land in the GBA is developing towards a more intensive direction.

From the perspective of the change in the PARA-MN of urban forms, there is generally less spatial difference (Fig. 7d). From the perspective of the cumulative changes in four periods, 50 % of counties had an increasing PARA-MN, while 50 % had a decreasing PARA-MN. The three counties with the largest increases in PARA-MN were Xinhui, Haizhu, and Shunde, with changes of 69.61, 67.94, and 50.66, respectively. The three counties with the largest decreases in PARA-MN were Liwan, Longgang, and Yantian, with changes
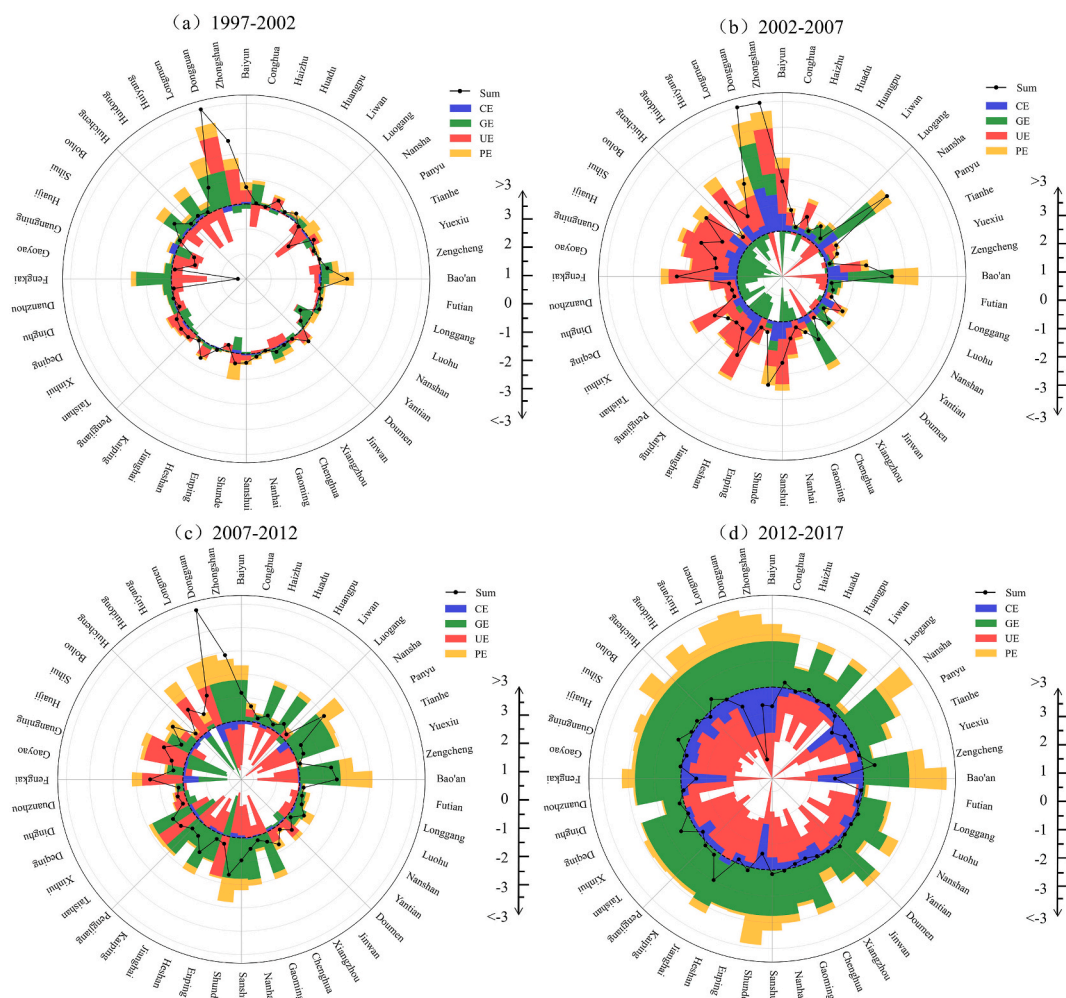
Fig. 6. The decomposition of carbon emission factors and the sum of contribution values of each factor in the GBA from 1997 to 2017. (a)–(d) show the factor contribution values and sum in 1997–2002 (a), 2002–2007 (b), 2007–2012 (c), and 2012–2017 (d).

of −176.38, −143.97, and −111.23, respectively. This indicates that the complexity of the urban forms in counties in the GBA has not changed dramatically with the rapid urban expansion, and the differences between counties are not large.

4.5. The relationship between urban form changes and carbon emissions

4.5.1. Identification and prevention of multicollinearity

To ensure the quality and robustness of the regression model, it is necessary to test the four explanatory variables of ΔNP, ΔLPI, ΔCOHESION, and ΔPARA-MN for multicollinearity. Fig. 8 shows the relationships between the four explanatory variables in four periods from 1997 to 2002, 2002–2007, 2007–2012, and 2012–2017. The correlations between the four explanatory variables are relatively low. Table 3 shows the variance inflation factors (VIF) of the explanatory variables. The VIF values of all the explanatory variables are less than 7.5, and the 1/VIF values are all greater than 0.1. This indicates that there is no multicollinearity between the explanatory variables.

4.5.2. Model performance comparison and testing

As shown in Table 4, the R^2 and Adj. R^2 of the MGWR model are generally higher than those of the traditional GWR model, while the AICc and RMSE of the MGWR model are both lower than those of the GWR model. This indicates that the MGWR model has better estimation performance in detecting the spatial relationship between urban form change and carbon emissions.

To determine whether the MGWR model is well-behaved, this study examined the distribution of the standardized residuals of the regression model (Table 5). The mean is close to 0, the standard deviation is close to 1, and it basically conforms to the normal distribution. Furthermore, the spatial autocorrelation (Global Moran's I) of the regression residuals was tested (Table 6), and there is no significant clustering of high or low residuals. This indicates that the MGWR model performs well.

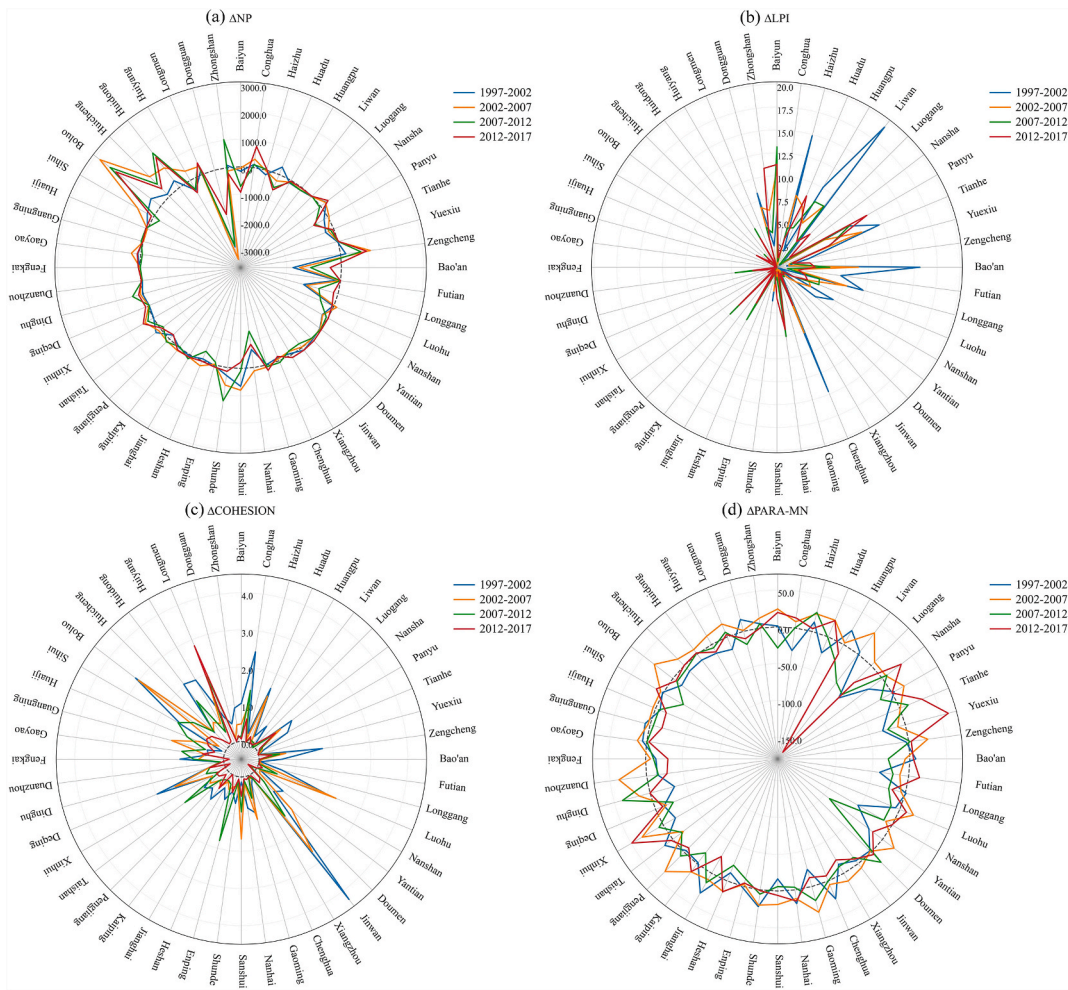**Fig. 7.** Changes of urban form in the GBA from 1997 to 2017. (a)-(d)show the changes of NP(a), LPI(b), COHESION(c), and PARA-MN(d).
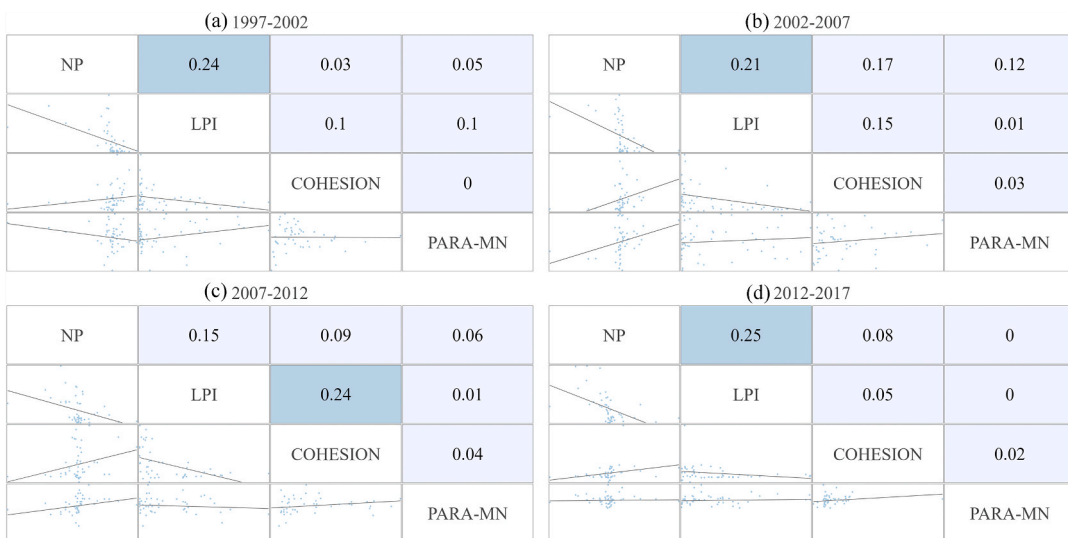
Fig. 8. Scatter plots of the relationships between the four explanatory variables of ΔNP, ΔLPI, ΔCOHESION, and ΔPARA-MN, with R^2 values shown in the upper left corner. (a)–(d) show the relationships and R^2 values in 1997–2002 (a), 2002–2007 (b), 2007–2012 (c), and 2012–2017 (d).

Table 3
Variance inflation factors of ΔNP, ΔLPI, ΔCOHESION, and ΔPARA-MN.

Variable	1997–2002		2002–2007		2007–2012		2012–2017	
	VIF	1/VIF	VIF	1/VIF	VIF	1/VIF	VIF	1/VIF
ΔNP	1.33	0.75	1.5	0.66	1.37	0.73	1.36	0.73
ΔLPI	1.53	0.65	1.65	0.61	1.44	0.70	1.39	0.72
ΔPARA-MN	1.14	0.88	1.3	0.77	1.26	0.79	1.12	0.89
ΔCOHESION	1.13	0.89	1.27	0.79	1.09	0.91	1.03	0.97

Table 4
Comparison of model performance between GWR and MGWR.

	Variable	CE		GE		UE		PE	
	Model	GWR	MGWR	GWR	MGWR	GWR	MGWR	GWR	MGWR
1997–2002	R^2	0. 39	0.34	0. 22	0.61	0.18	0.26	0.19	0.72
	Adj. R^2	0.24	0.22	0.09	0.45	0.05	0.13	0.07	0.58
	AICc	136.15	135.90	141.37	135.31	143.35	141.37	142.14	128.01
	RMSE	0.76	0.77	0.90	0.55	0.95	0.87	0.93	0.41
2002–2007	R^2	0.20	0.67	0.61	0.77	0.44	0.65	0.19	0.55
	Adj. R^2	0.08	0.52	0.47	0.68	0.33	0.55	0.06	0.41
	AICc	141.03	132.44	121.08	106.36	128.12	116.67	143.02	130.32
	RMSE	0.92	0.48	0.51	0.32	0.67	0.45	0.94	0.58
2007–2012	R^2	0.31	0.43	0.68	0.79	0.42	0.82	0.27	0.55
	Adj. R^2	0.18	0.30	0.51	0.68	0.34	0.72	0.09	0.43
	AICc	136.71	133.71	128.69	115.22	125.28	108.02	144.44	126.39
	RMSE	0.81	0.69	0.48	0.32	0.66	0.27	0.90	0.57
2012–2017	R^2	0.52	0.75	0.08	0.67	0.08	0.66	0.36	0.52
	Adj. R^2	0.35	0.63	−0.04	0.54	−0.04	0.52	0.20	0.36
	AICc	134.71	123.17	147.04	125.78	147.08	127.64	139.23	137.29
	RMSE	0.65	0.37	1.03	0.46	1.04	0.48	0.80	0.64

Table 5
Distribution of standardized residuals.

	Variable	CE	GE	UE	PE
1997–2002	Mean	0.14	0.09	−0.16	−0.04
	Std	0.98	1.01	0.98	1.16
2002–2007	Mean	0.1	−0.04	0.13	−0.03
	Std	1.11	1.08	1.01	1
2007–2012	Mean	−0.01	−0.3	0	−0.01
	Std	1	0.97	1.02	1.03
2012–2017	Mean	0.1	0.07	−0.07	−0.07
	Std	1.17	1.07	1.06	1.04

Table 6
Spatial autocorrelation of regression residuals.

	Variable	CE	GE	UE	PE
1997–2002	Moran's I	0.01	−0.19	−0.07	−0.16
	z-score	0.08	−1.75	−0.56	−1.36
	p-value	0.93	0.08	0.58	0.17
2002–2007	Moran's I	−0.16	−0.08	−0.16	−0.02
	z-score	−1.26	−0.64	−1.39	0.01
	p-value	0.2	0.52	0.16	1
2007–2012	Moran's I	−0.14	−0.2	−0.02	−0.04
	z-score	−1.16	−1.71	0.02	−0.14
	p-value	0.25	0.09	0.98	0.89
2012–2017	Moran's I	−0.14	−0.08	−0.09	−0.12
	z-score	−1.18	−0.56	−0.67	−0.92
	p-value	0.24	0.58	0.5	0.36

4.5.3. MGWR model results analysis

The impact of urban form changes on carbon emissions in the four periods of 1997–2002, 2002–2007, 2007–2012, and 2012–2017 is shown in Fig. 9. ΔNP, ΔLPI, and ΔCOHESION have a significant impact on carbon emissions in the GBA, while ΔPARA-MN has no
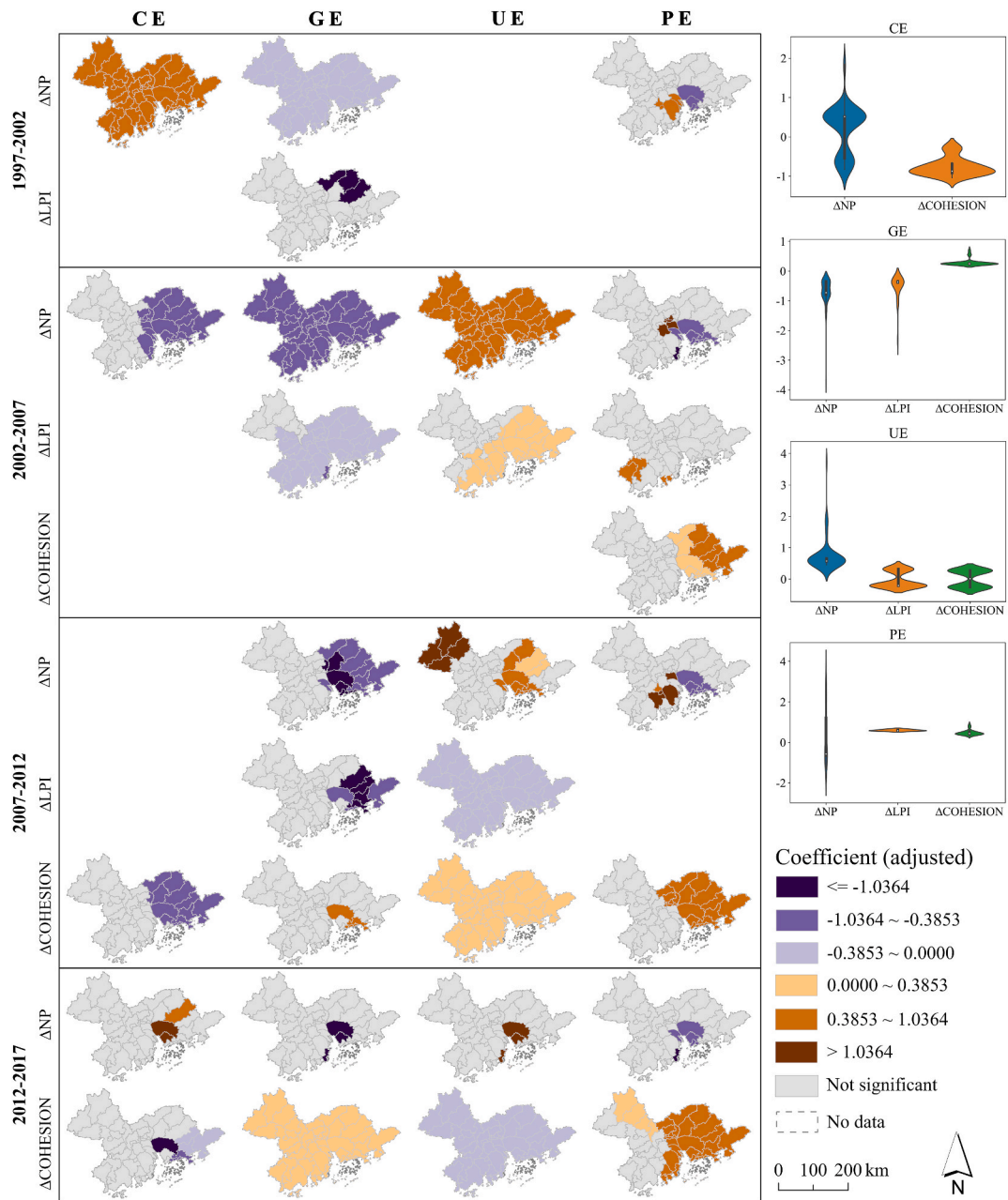
Fig. 9. Spatial distribution of regression coefficients of urban form changes and carbon emission driving factors depicted using MGWR in the four periods of 1997–2002, 2002–2007, 2007–2012, and 2012–2017. Local significance (95 % confidence) is controlled by t-value. Results that are globally insignificant in a single period are not shown; violin plots show the distribution of regression coefficients that are significant (95 % confidence).

significant impact on carbon emissions in all counties in any of the four periods.

In the period 1997–2002, ΔNP and ΔLPI had an impact on CE, GE, and PE. ΔNP was positively correlated with CE in the entire GBA, with an average coefficient of 0.52. ΔNP and ΔLPI were negatively correlated with GE, with ΔNP having a wider range of impact than ΔLPI but a lower magnitude. The average coefficient for ΔNP was −0.35, and for ΔLPI it was −2.13. The impact of ΔNP on PE was differentiated along the Pearl River Estuary, with a negative correlation on the east coast and a positive correlation on the west coast.

Moving to the period 2002–2007, ΔNP, ΔLPI, and ΔCOHESION affected carbon emissions. ΔNP was negatively correlated with CE and GE, positively correlated with UE globally, and showed significant spatial variation in its impact on PE. ΔNP's impact on CE was concentrated in the eastern region of the GBA, with an average coefficient of −0.63. ΔLPI was negatively correlated with GE, positively correlated with UE and PE, with average coefficients of −0.36 and 0.35, respectively. ΔCOHESION was only positively correlated in

the eastern region of the GBA.

For the period 2007–2012, ΔNP, ΔLPI, and ΔCOHESION exhibited impacts on carbon emissions. ΔNP demonstrated a strong negative correlation with GE in the eastern GBA, a positive correlation with UE, while its impact on PE varied along the coast of the Pearl River Estuary. The average coefficient of ΔNP for GE was −1.08 and for UE was 0.88. ΔLPI showed a localized negative correlation with GE in the eastern GBA and a global negative correlation with UE, with average coefficients of −0.32 for both. ΔCOHESION displayed a localized negative correlation with CE in the eastern GBA, while showing localized positive correlations with GE and PE. It exhibited a global positive correlation with UE. The average coefficient for ΔCOHESION with CE was −0.82, and with GE and PE, it was 0.5.

Finally, in the period 2012–2017, ΔNP and ΔCOHESION had significant impacts on carbon emissions. The influence of ΔNP was primarily concentrated along the coast of the Pearl River Estuary. It exhibited a positive correlation with CE and UE, and a negative correlation with GE and PE, with average coefficients of 1.78 and −1.24, respectively. ΔCOHESION exerted a global impact on GE and UE, while having localized effects on CE and PE. It demonstrated a negative correlation with CE and UE, and a positive correlation with GE and PE, with average coefficients of −0.32 and 0.35, respectively.

5. Discussion

5.1. The impact of urban expansion on carbon emissions

There is a strong correlation between urban expansion and carbon emissions in the GBA. During the period 1997–2017, carbon emissions in the GBA's counties experienced a period of rapid growth followed by a gradual slowdown, which was closely related to urban expansion. For the GBA, 2012 was a critical juncture, which can be attributed to the transformation of development concepts leading to industrial structure adjustment and restrictions on urban expansion [30,52]. After 2012, carbon emissions and urban expansion entered a stage of coordinated development, which is to generally achieve decoupling of urban expansion and carbon emissions, although this coordinated relationship is still unstable, especially in 2014 and 2016 when there were uncoordinated situations (Fig. 4), which is related to the growth of carbon emissions in those years (Fig. 2). Economically developed areas and regions with key environmental protection are more likely to achieve coordinated development of urban expansion and carbon emissions (Fig. 5), which reflects the advantages and potential of optimizing the economic development model and strict environmental protection measures in achieving carbon neutrality [53–56]. As shown in Fig. 6 and Table 7, the GE and UE in the GBA have the greatest impact on carbon emissions, both of which are related to the area of urban expansion. In the coordinated stage of urban expansion and carbon emissions (after 2012), the GE and PE promote the growth of carbon emissions, while the CE and UE can inhibit the growth of carbon emissions. In terms of inhibiting carbon emissions, the contribution rate of controlling urban land is as high as 86 %. Although economic development in the GBA is dependent on carbon emissions, reasonable control of urban expansion can significantly offset the negative impact of this dependence.

5.2. The impact of urban form changes on carbon emissions

The changes in urban form in the GBA's counties have an impact on carbon emissions. The ΔNP has significant spatial differences (Fig. 9). The counties of Dongguan and Shenzhen have been continuously declining. Combined with Fig. 6, the decline in NP in Dongguan and Shenzhen will promote carbon emissions. Although some studies have shown that carbon emissions will increase with the increase in urban land fragmentation [23,27]. However, considering the function and economic development of the region, the increase in fragmentation can reduce carbon emissions [57]. Therefore, it is appropriate to consider dispersing urban land, easing urban functions and population, to reduce carbon emissions in Dongguan and Shenzhen. The LPI of the GBA is increasing (Fig. 9), but this increase has a more significant impact on the carbon emissions of Dongguan, Shenzhen and Huizhou counties. This trend of single-core development will weaken the economic effect, thereby reducing carbon emissions. This impact reached its peak in 2007–2012, with an average coefficient of 0.9. After that, its impact was no longer significant. In general, the COHESION of county-level cities is increasing (Fig. 9). This enhancement mainly focuses on two periods after 2007. In 2012–2017, the increase in COHESION will increase the GE and PE, and reduce the CE and UE. That is, the increase in compactness has a two-sided impact on carbon emissions [26,32]. However, for the counties in the eastern part of the GBA, Zhongshan and Zhuhai, the increase in COHESION will increase the PE, leading to an increase in carbon emissions. In general, the spatial differences in Δ PARA - MN are not large (Fig. 9). Although some studies have shown that the increase in urban form complexity has an adverse impact on carbon emissions [32,58], the MGWR model used in this study did not capture the significant impact of Δ PARA - MN on carbon emission drivers.

Table 7
Total contribution values of carbon emission driving factors.

	CE	GE	UE	PE	Sum
1997–2002	0.03	21.27	−23.77	22.10	19.62
2002–2007	36.54	9.48	44.58	22.40	112.99
2007–2012	−10.26	95.59	−43.67	33.16	74.81
2012–2017	−68.46	456.60	−435.86	37.04	−10.68

6. Conclusion

This study investigated the relationship between urban expansion and morphological changes at the county level in the Bay Area over the past 20 years (1997–2017). The main conclusions are as follows.

(1) Urban expansion and carbon emissions in the GBA have gone through three stages. After 2012, urban expansion and carbon emissions entered a coordinated development stage. The optimization of economic development models and strict environmental protection measures can promote carbon neutrality. The GE and PE have become the main factors promoting carbon emissions growth, while CE and UE have become the main factors restraining carbon emissions growth. In terms of restraining carbon emissions, the contribution rate of controlling urban land is as high as 86 %.

(2) The relationship between urban form changes and carbon emissions at the county level in the GBA has temporal and spatial differences. The continuous decline in urban fragmentation in Dongguan and Shenzhen has indirectly increased carbon emissions. The increase in centrality indicates that the trend of single-core development in county-level cities in the Bay Area has strengthened. In 2007–2012, it reached its peak in terms of its positive impact on carbon emissions in Dongguan, Shenzhen, and Huizhou counties. The increase in compactness has had a significant impact on carbon emissions in the GBA since 2007, although this impact has two sides. However, in the eastern part of the GBA, Zhongshan and Zhuhai, it is not conducive to reducing carbon emissions.

The study has some limitations: First, the data formats used are different. Carbon emission data come from panel data, while urban land, population, and economic data come from raster data. There is spatial inconsistency, which affects the accuracy of the study. Second, the study does not fully consider the impact of urban form on carbon emissions, and the impact of urban form complexity is not clear. In future studies, we will unify data formats, select more comprehensive carbon emission driving factors and indicators to characterize urban form changes, and establish a more comprehensive and detailed indicator system to further study the impact of urban expansion and form changes on carbon emissions. This will provide some scientific basis for the carbon neutrality goal of the GBA.

CRediT authorship contribution statement

Lei Ming: Writing – original draft, Methodology, Formal analysis, Data curation. **Yuandong Wang:** Supervision, Methodology, Funding acquisition, Conceptualization. **Xiaojie Chen:** Writing – review & editing, Validation. **Lihong Meng:** Writing – review & editing, Validation.

Declaration of competing interest

The authors declare that they have no known competing financial interests or personal relationships that could have appeared to influence the work reported in this paper.

Acknowledgments

References

[1] W. Fei, S. Zhao, Urban land expansion in China's six megacities from 1978 to 2015, Sci. Total Environ. 664 (2019) 60–71, https://doi.org/10.1016/j.scitotenv.2019.02.008.
[2] Y. Zhou, T. Wu, Y. Wang, Urban expansion simulation and development-oriented zoning of rapidly urbanising areas: a case study of Hangzhou, Sci. Total Environ. 807 (2022) 150813, https://doi.org/10.1016/j.scitotenv.2021.150813.
[3] W. Zhou, W. Yu, Y. Qian, L. Han, S.T.A. Pickett, J. Wang, W. Li, Z. Ouyang, Beyond city expansion: multi-scale environmental impacts of urban megaregion formation in China, Natl. Sci. Rev. 9 (2022) nwab107, https://doi.org/10.1093/nsr/nwab107.
[4] Y. Shan, Y. Guan, Y. Hang, H. Zheng, Y. Li, D. Guan, J. Li, Y. Zhou, L. Li, K. Hubacek, City-level emission peak and drivers in China, Sci. Bull. 67 (2022) 1910–1920, https://doi.org/10.1016/j.scib.2022.08.024.
[5] X. Duan, X. Li, W. Tan, R. Xiao, Decoupling relationship analysis between urbanization and carbon emissions in 33 African countries, Heliyon 8 (2022) e10423, https://doi.org/10.1016/j.heliyon.2022.e10423.
[6] L. Liu, L. Xun, Z. Wang, H. Liu, Y. Huang, K.B. Bedra, Peak carbon dioxide emissions Strategy based on the Gray model between carbon emissions and urban spatial expansion for a built-up area, Appl. Sci. 13 (2023) 187, https://doi.org/10.3390/app13010187.
[7] Q. Wang, Y. Xiao, Has urban construction land achieved low-carbon sustainable development? A case study of North China plain, China, Sustainability 14 (2022) 9434, https://doi.org/10.3390/su14159434.
[8] J. Wen, X. Chuai, S. Li, S. Song, Y. Li, M. Wang, S. Wu, Spatial heterogeneity of the carbon emission effect resulting from urban expansion among three coastal Agglomerations in China, Sustainability 11 (2019) 4590, https://doi.org/10.3390/su11174590.
[9] Z. Chang, S. Liu, Y. Wu, K. Shi, The regional disparity of urban spatial expansion is greater than that of urban socioeconomic expansion in China: a new perspective from nighttime light remotely sensed data and urban land datasets, Rem. Sens. 14 (2022) 4348, https://doi.org/10.3390/rs14174348.
[10] S.A.A. Rifat, W. Liu, Quantifying spatiotemporal patterns and major explanatory factors of urban expansion in Miami metropolitan area during 1992–2016, Rem. Sens. 11 (2019) 2493, https://doi.org/10.3390/rs11212493.
[11] Z. Wang, H. Fu, H. Liu, C. Liao, Urban development sustainability, industrial structure adjustment, and land use efficiency in China, Sustain. Cities Soc. 89 (2023) 104338, https://doi.org/10.1016/j.scs.2022.104338.

[12] R. Wu, Z. Li, S. Wang, The varying driving forces of urban land expansion in China: insights from a spatial-temporal analysis, Sci. Total Environ. 766 (2021) 142591, https://doi.org/10.1016/j.scitotenv.2020.142591.

[13] Y. Yi, J. Qi, D. Chen, Impact of population agglomeration in big cities on carbon emissions, Environ. Sci. Pollut. Res. 29 (2022) 86692–86706, https://doi.org/10.1007/s11356-022-21722-9.

[14] T. Zhang, Y. Song, J. Yang, Relationships between urbanization and CO2 emissions in China: an empirical analysis of population migration, PLoS One 16 (2021) e0256335, https://doi.org/10.1371/journal.pone.0256335.

[15] L. Lai, X. Huang, H. Yang, X. Chuai, M. Zhang, T. Zhong, Z. Chen, Y. Chen, X. Wang, J.R. Thompson, Carbon emissions from land-use change and management in China between 1990 and 2010, Sci. Adv. 2 (2016) e1601063, https://doi.org/10.1126/sciadv.1601063.

[16] J. Chen, C. Xu, M. Song, Determinants for decoupling economic growth from carbon dioxide emissions in China, Reg. Environ. Change 20 (2020) 11, https://doi.org/10.1007/s10113-020-01605-w.

[17] Z. Wei, K. Wei, J. Liu, Decoupling relationship between carbon emissions and economic development and prediction of carbon emissions in Henan Province: based on Tapio method and STIRPAT model, Environ. Sci. Pollut. R. 30 (2023) 52679–52691, https://doi.org/10.1007/s11356-023-26051-z.

[18] J.R. Alaganthiran, M.I. Anaba, The effects of economic growth on carbon dioxide emissions in selected Sub-Saharan African (SSA) countries, Heliyon 8 (2022) e11193, https://doi.org/10.1016/j.heliyon.2022.e11193.

[19] W. Sun, C. Huang, How does urbanization affect carbon emission efficiency? Evidence from China, J. Clean. Prod. 272 (2020) 122828, https://doi.org/10.1016/j.jclepro.2020.122828.

[20] Y. Wang, J. Liu, J. Wang, Z. Liu, Exploring the effect of city size on carbon emissions: evidence from 259 prefecture-level cities in China, Environ. Sci. Pollut. Res. Int. (2023), https://doi.org/10.1007/s11356-023-28564-z.

[21] C. Li, Y. Li, K. Shi, Q. Yang, A multiscale evaluation of the coupling relationship between urban land and carbon emissions: a case study of chongqing, China, Int. J. Environ. Res. Publ. Health 17 (2020) 3416, https://doi.org/10.3390/ijerph17103416.

[22] S. Zheng, Y. Huang, Y. Sun, Effects of urban form on carbon emissions in China: implications for low-carbon urban planning, Land 11 (2022) 1343, https://doi.org/10.3390/land11081343.

[23] J. Ou, X. Liu, X. Li, Y. Chen, Quantifying the relationship between urban forms and carbon emissions using panel data analysis, Landsc. Ecol. 28 (2013) 1889–1907, https://doi.org/10.1007/s10980-013-9943-4.

[24] H. Shunfa, E.C. Hui, L. Yaoyu, Relationship between urban spatial structure and carbon emissions: a literature review, Ecol. Indicat. 144 (2022) 109456, https://doi.org/10.1016/j.ecolind.2022.109456.

[25] M. Cai, C. Ren, Y. Shi, G. Chen, J. Xie, E. Ng, Modeling spatiotemporal carbon emissions for two mega-urban regions in China using urban form and panel data analysis, Sci. Total Environ. 857 (2023) 159612, https://doi.org/10.1016/j.scitotenv.2022.159612.

[26] G. Ding, J. Guo, S.G. Pueppke, J. Yi, M. Ou, W. Ou, Y. Tao, The influence of urban form compactness on CO2 emissions and its threshold effect: evidence from cities in China, J. Environ. Manag. 322 (2022) 116032, https://doi.org/10.1016/j.jenvman.2022.116032.

[27] K. Shi, T. Xu, Y. Li, Z. Chen, W. Gong, J. Wu, B. Yu, Effects of urban forms on CO2 emissions in China from a multi-perspective analysis, J. Environ. Manag. 262 (2020) 110300, https://doi.org/10.1016/j.jenvman.2020.110300.

[28] H. Wu, S. Fang, C. Zhang, S. Hu, D. Nan, Y. Yang, Exploring the impact of urban form on urban land use efficiency under low-carbon emission constraints: a case study in China's Yellow River Basin, J. Environ. Manag. 311 (2022) 114866, https://doi.org/10.1016/j.jenvman.2022.114866.

[29] Y. Wu, C. Li, K. Shi, S. Liu, Z. Chang, Exploring the effect of urban sprawl on carbon dioxide emissions: an urban sprawl model analysis from remotely sensed nighttime light data, Environ. Impact Assess. Rev. 93 (2022) 106731, https://doi.org/10.1016/j.eiar.2021.106731.

[30] X. Liu, H. Xu, M. Zhang, The effects of urban expansion on carbon emissions: based on the spatial interaction and transmission mechanism, J. Clean. Prod. 434 (2024) 140019, https://doi.org/10.1016/j.jclepro.2023.140019.

[31] S. Wang, C. Fang, Y. Wang, Y. Huang, H. Ma, Quantifying the relationship between urban development intensity and carbon dioxide emissions using a panel data analysis, Ecol. Indicat. 49 (2015) 121–131, https://doi.org/10.1016/j.ecolind.2014.10.004.

[32] C. Fang, S. Wang, G. Li, Changing urban forms and carbon dioxide emissions in China: a case study of 30 provincial capital cities, Appl. Energy 158 (2015) 519–531, https://doi.org/10.1016/j.apenergy.2015.08.095.

[33] J. Chen, M. Gao, S. Cheng, W. Hou, M. Song, X. Liu, Y. Liu, Y. Shan, County-level CO2 emissions and sequestration in China during 1997–2017, Sci. Data 7 (2020) 391, https://doi.org/10.1038/s41597-020-00736-3.

[34] P. Gong, X. Li, J. Wang, Y. Bai, B. Chen, T. Hu, X. Liu, B. Xu, J. Yang, W. Zhang, Y. Zhou, Annual maps of global artificial impervious area (GAIA) between 1985 and 2018, Remote Sens. Environ. 236 (2020) 111510, https://doi.org/10.1016/j.rse.2019.111510.

[35] A.E. Gaughan, F.R. Stevens, C. Linard, P. Jia, A.J. Tatem, High resolution population distribution maps for southeast Asia in 2010 and 2015, PLoS One 8 (2013) e55882, https://doi.org/10.1371/journal.pone.0055882.

[36] J. Chen, M. Gao, S. Cheng, W. Hou, M. Song, X. Liu, Y. Liu, Global 1 km × 1 km gridded revised real gross domestic product and electricity consumption during 1992–2019 based on calibrated nighttime light data, Sci. Data 9 (2022) 202, https://doi.org/10.1038/s41597-022-01322-5.

[37] P. Tapio, Towards a theory of decoupling: degrees of decoupling in the EU and the case of road traffic in Finland between 1970 and 2001, Transport Pol. 12 (2005) 137–151, https://doi.org/10.1016/j.tranpol.2005.01.001.

[38] S. Lundquist, Explaining events of strong decoupling from CO2 and NOx emissions in the OECD 1994–2016, Sci. Total Environ. 793 (2021) 148390, https://doi.org/10.1016/j.scitotenv.2021.148390.

[39] B. Liu, Y. Guan, Y. Shan, C. Cui, K. Hubacek, Emission growth and drivers in Mainland Southeast Asian countries, J. Environ. Manag. 329 (2023) 117034, https://doi.org/10.1016/j.jenvman.2022.117034.

[40] L. Yang, Y. Yang, H. Lv, D. Wang, Whether China made efforts to decouple economic growth from CO2 emissions?-Production vs consumption perspective, Environ. Sci. Pollut. R. 27 (2020) 5138–5154, https://doi.org/10.1007/s11356-019-07317-x.

[41] Y. Wu, Q. Zhu, B. Zhu, Decoupling analysis of world economic growth and CO2 emissions: a study comparing developed and developing countries, J. Clean. Prod. 190 (2018) 94–103, https://doi.org/10.1016/j.jclepro.2018.04.139.

[42] X. Zhao, X. Zhang, S. Shao, Decoupling CO2 emissions and industrial growth in China over 1993–2013: the role of investment, Energy Econ. 60 (2016) 275–292, https://doi.org/10.1016/j.eneco.2016.10.008.

[43] B.W. Ang, LMDI decomposition approach: a guide for implementation, Energy Pol. 86 (2015) 233–238, https://doi.org/10.1016/j.enpol.2015.07.007.

[44] Z. Akyürek, LMDI decomposition analysis of energy consumption of Turkish manufacturing industry: 2005–2014, Energy Effic 13 (2020) 649–663, https://doi.org/10.1007/s12053-020-09846-8.

[45] B.W. Ang, K.-H. Choi, Decomposition of aggregate energy and gas emission intensities for industry: a refined divisia index method, Energy J. 18 (1997) 59–73, https://doi.org/10.5547/ISSN0195-6574-EJ-Vol18-No3-3.

[46] C. Wang, K. Wu, X. Zhang, F. Wang, H. Zhang, Y. Ye, Q. Wu, G. Huang, Y. Wang, B. Wen, Features and drivers for energy-related carbon emissions in mega city: the case of Guangzhou, China based on an extended LMDI model, PLoS One 14 (2019) e0210430, https://doi.org/10.1371/journal.pone.0210430.

[47] Y. Liu, J. Wu, D. Yu, Q. Ma, The relationship between urban form and air pollution depends on seasonality and city size, Environ. Sci. Pollut. R. 25 (2018) 15554–15567, https://doi.org/10.1007/s11356-018-1743-6.

[48] Y. Jia, L. Tang, M. Xu, X. Yang, Landscape pattern indices for evaluating urban spatial morphology – a case study of Chinese cities, Ecol. Indicat. 99 (2019) 27–37, https://doi.org/10.1016/j.ecolind.2018.12.007.

[49] H. Yu, A.S. Fotheringham, Z. Li, T. Oshan, W. Kang, L.J. Wolf, Inference in multiscale geographically weighted regression, Geogr. Anal. 52 (2020) 87–106, https://doi.org/10.1111/gean.12189.

[50] X. Song, N. Mi, W. Mi, L. Li, Spatial non-stationary characteristics between grass yield and its influencing factors in the Ningxia temperate grasslands based on a mixed geographically weighted regression model, J. Geogr. Sci. 32 (2022) 1076–1102, https://doi.org/10.1007/s11442-022-1986-5.

[51] L. Zhou, W. Xiao, Z. Zheng, H. Zhang, Commercial dynamics in urban China during the COVID-19 recession: vulnerability and short-term adaptation of commercial centers in Shanghai, Appl. Geogr. 152 (2023) 102889, https://doi.org/10.1016/j.apgeog.2023.102889.

[52] J. Zheng, Z. Mi, D. Coffman, S. Milcheva, Y. Shan, D. Guan, S. Wang, Regional development and carbon emissions in China, Energy Econ. 81 (2019) 25–36, https://doi.org/10.1016/j.eneco.2019.03.003.

[53] Q. Wang, F. Zhang, The effects of trade openness on decoupling carbon emissions from economic growth – evidence from 182 countries, J. Clean. Prod. 279 (2021) 123838, https://doi.org/10.1016/j.jclepro.2020.123838.

[54] Q. Wang, R. Jiang, Is China's economic growth decoupled from carbon emissions? J. Clean. Prod. 225 (2019) 1194–1208, https://doi.org/10.1016/j.jclepro.2019.03.301.

[55] H. Wu, L. Xu, S. Ren, Y. Hao, G. Yan, How do energy consumption and environmental regulation affect carbon emissions in China? New evidence from a dynamic threshold panel model, Resour. Pol. 67 (2020) 101678, https://doi.org/10.1016/j.resourpol.2020.101678.

[56] Y.-J. Zhang, Y.-L. Peng, C.-Q. Ma, B. Shen, Can environmental innovation facilitate carbon emissions reduction? Evidence from China, Energy Pol. 100 (2017) 18–28, https://doi.org/10.1016/j.enpol.2016.10.005.

[57] S. Zuo, S. Dai, Y. Ren, More fragmentized urban form more CO2 emissions? A comprehensive relationship from the combination analysis across different scales, J. Clean. Prod. 244 (2020) 118659, https://doi.org/10.1016/j.jclepro.2019.118659.

[58] S. Wang, J. Wang, C. Fang, S. Li, Estimating the impacts of urban form on CO2 emission efficiency in the Pearl River Delta, China, Cities 85 (2019) 117–129, https://doi.org/10.1016/j.cities.2018.08.009.